History of expansion and anthropogenic collapse in a top marine predator of the Black Sea estimated from genetic data

Michaël C. Fontaine[a,b,1], Alodie Snirc[a], Alexandros Frantzis[c], Emmanuil Koutrakis[d], Bayram Öztürk[e], Ayaka A. Öztürk[e], and Fréderic Austerlitz[a,b]

[a]Laboratoire d'Ecologie, Systématique et Evolution, Unité Mixte de Recherche 8079, Université Paris-Sud–Centre National de la Recherche Scientifique–AgroParisTech, 91405 Orsay, France; [b]Eco-Anthropologie et Ethnobiologie, Unité Mixte de Recherche 7206, Centre National de la Recherche Scientifique–Muséum National d'Histoire Naturelle–Université Paris Diderot–Sorbonne Paris Cité, 75005 Paris, France; [c]Pelagos Cetacean Research Institute, 16671 Vouliagmeni, Greece; [d]Fisheries Research Institute, Hellenic Agricultural Organization–Demeter, Nea Peramos, 64007 Kavala, Greece; and [e]Faculty of Fisheries, Istanbul University, TR-34320 Laleli-Istanbul, Turkey

Edited by David M. Karl, University of Hawaii, Honolulu, HI, and approved July 20, 2012 (received for review February 17, 2012)

Two major ecological transitions marked the history of the Black Sea after the last Ice Age. The first was the postglacial transition from a brackish-water to a marine ecosystem dominated by porpoises and dolphins once this basin was reconnected back to the Mediterranean Sea (*ca.* 8,000 y B.P.). The second occurred during the past decades, when overfishing and hunting activities brought these predators close to extinction, having a deep impact on the structure and dynamics of the ecosystem. Estimating the extent of this decimation is essential for characterizing this ecosystem's dynamics and for formulating restoration plans. However, this extent is poorly documented in historical records. We addressed this issue for one of the main Black Sea predators, the harbor porpoise, using a population genetics approach. Analyzing its genetic diversity using an approximate Bayesian computation approach, we show that only a demographic expansion (at most 5,000 y ago) followed by a contemporaneous population collapse can explain the observed genetic data. We demonstrate that both the postglacial settlement of harbor porpoises in the Black Sea and the recent anthropogenic activities have left a clear footprint on their genetic diversity. Specifically, we infer a strong population reduction (~90%) that occurred within the past 5 decades, which can therefore clearly be related to the recent massive killing of small cetaceans and to the continuing incidental catches in commercial fisheries. Our study thus provides a quantitative assessment of these demographically catastrophic events, also showing that two separate historical events can be inferred from contemporary genetic data.

conservation biology | demographic inference | coalescence | Bayesian analyses

The Black Sea is a deep, mostly land-locked basin in Eastern Europe, linked to the Mediterranean Sea by the narrow straits of Bosporus and Dardanelles (Fig. 1). Described as a healthy ecosystem dominated by various marine predators during the Antiquity (1), the Black Sea has undergone dramatic changes in recent decades. Among these major anthropogenic impacts are fish stock collapses, eutrophication, and invasion by alien species. Initially, most of these ecosystem changes were attributed solely to eutrophication (2, 3). However, hydrological and climate changes (4, 5), predation effects, and fishing (6–8) have recently been recognized as other important contributing factors. These changes, together with the relatively simple trophic food-web in the Black Sea, make this ecosystem an attractive "natural laboratory" for studying ecosystem dynamics, regime shifts, and trophic interactions (7–10).

Apex marine predators are a key component of this ecosystem, because they regulate the demography of species at lower trophic levels through a top-down regulation of the trophic food-web (4, 7, 8, 11). Modeling studies have suggested that the recent decimation of these predators in the Black Sea was a key factor in reducing ecosystem resilience, inevitably leading to its reorganization (i.e., a regime shift) (7, 8, 10, 11). Since the 1960s, the abundance of planktivorous fish has progressively increased, following the sharp decline of pelagic predators. As a response to increased planktivory, zooplankton decreased and so, in turn, did their grazing pressure on phytoplankton. The combination of favorable climatic influences, nutrient enrichment from land-based sources, and low grazing pressure on phytoplankton led to intense eutrophication (7), including the development of massive algal blooms events (red tides) reported during the 1980s (2, 3).

Three cetacean species, the harbor porpoise (*Phocoena phocoena*), the short-beaked common dolphin (*Delphinus delphis*), and the common bottlenose dolphin (*Tursiops truncatus*), crown the trophic food-web of the Black Sea as top predators, with no natural predators in this basin (12–14). By the early 1970s, dolphin fisheries had dramatically reduced populations of these small cetaceans. Estimates, based on fishery records from Turkey only, suggest that up to 176,000 animals were killed annually, of which more than half were harbor porpoises (15, 16). Because of this severe abundance decline, hunting of small cetaceans was banned in Bulgaria, Romania, and the former Union of Soviet Socialist Republics in 1966 but continued in Turkey until 1983, with some illegal hunting reported until 1991. Currently, incidental mortality in fishing nets has replaced direct hunting as the main threat for small cetaceans, killing thousands of animals each year, with the overwhelming majority (>95%) being harbor porpoises (15). Hence, it is clear that natural populations of small cetaceans, particularly of harbor porpoises, have become severely depleted over the past 50 y (15). However, the exact magnitude of the abundance declines of these small cetaceans remains largely unknown. According to historical records, at least 70% of the harbor porpoise population could have been lost (15), but this value is highly uncertain due to the absence of information on the predecline abundances of these populations and on the mortality caused directly, or indirectly, by the fisheries (15). However, such information is crucial for modeling ecosys-

Author contributions: M.C.F. designed research; M.C.F. and A.S. performed research; A.F., E.K., B.Ö., A.A.Ö., and F.A. contributed new reagents/analytic tools; M.C.F., A.S., and F.A. analyzed data; and M.C.F. and F.A. wrote the paper.

The authors declare no conflict of interest.

This article is a PNAS Direct Submission.

Data deposition: Sequence and genotype data from this project are deposited at DRYAD (http://dx.doi.org/10.5061/dryad.km038) and at GenBank (accession nos. JX105486–JX105517).

See Commentary on page 15078.

[1]To whom correspondence should be addressed. E-mail: mikafontaine@gmail.com.

See Author Summary on page 15099 (volume 109, number 38).

This article contains supporting information online at www.pnas.org/lookup/suppl/doi:10.1073/pnas.1201258109/-/DCSupplemental.

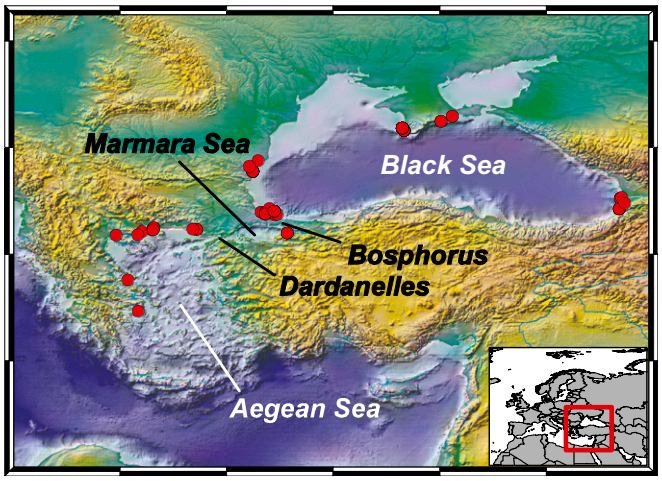

Fig. 1. Maps show the sampling locations indicated by red dots. *Inset* shows area of the main map.

tem dynamics (7, 8, 11) and ecosystem restoration (17, 18). Ecosystem restoration may require that threatened populations of ecologically pivotal species recover to their former abundances, but it is often difficult to estimate the historic population size of heavily exploited species (17, 18).

Variation in the abundance of individuals also affects the dynamics of the genes carried by these individuals. Hence, a powerful alternative to direct abundance estimation is the use of population genetics methods to draw inferences on past demography using the observed distribution of genetic variation in contemporary populations (19, 20). In particular, some of these approaches use coalescent theory in a specific demographic model, which assumes that the study population increased or decreased in size at a given moment in the past (21, 22) and aims to estimate the timing and intensity of such population size changes. An important assumption of these models is that the study population is isolated, such that changes in genetic diversity over time will only reflect changes in local effective population size (i.e., mainly change in the number of reproducing individuals) (23). For the three small cetaceans of the Black Sea, this assumption is likely only to be met by the harbor porpoise, which is both geographically and genetically isolated from the North Atlantic populations by the Mediterranean Sea (24–26). This isolated status has been the basis for recognizing the Black Sea harbor porpoise as a subspecies (*P. phocoena relicta*) distinct from the Atlantic subspecies (*P. phocoena phocoena*) (25), and it has also been instrumental to the species' current listing as endangered by the International Union for Conservation of Nature (15). During the most recent period of postglacial warming, harbor porpoises were displaced from the Mediterranean Sea into habitats where environmental conditions were still favorable, in the eastern North Atlantic and the Black Sea, where they founded a relict population (27). Currently, harbor porpoises are also reported in the northern Aegean Sea (Fig. 1), but it remains unknown whether they are part of the Black Sea population or a demographically distinct unit (28, 29).

In this study, we aimed to infer the demographic history of this endangered species from contemporary genetic data. Specifically, we use coalescent-based methods to infer both the timing and intensity of demographic events (i.e., the extent to which this population increased or decreased in size). Because such parameters cannot be inferred from climatic or historical records, genetic data can provide a valuable insight in this context. For this purpose, we evaluated the genetic polymorphism of harbor porpoises in the Black Sea and Aegean Sea at 10 nuclear autosomal microsatellite loci and at a fragment of the mitochondrial control region (mtDNA-CR). We analyzed these data using an approximate Bayesian computation (ABC) approach (30) to identify the demographic scenario that best fits with the data and to estimate the parameters of interest (timing and intensity of population size changes) under this scenario. The ABC approach is a suitable and powerful approach in such situations because it allows comparison of the probability of obtaining the observed data (or summary statistics computed from them) under various alternative scenarios (31, 32).

Results

Genetic Variation at the mtDNA-CR. A total of 705 base pairs from the mtDNA-CR were sequenced for 64 animals (10 from the Aegean Sea and 54 from the Black Sea; Fig. 1). Thirty-two distinct haplotypes were identified (*SI Appendix*, Table S1), with a haplotypic diversity ($H_d \pm$ SD) of 0.902 ± 0.031 and a nucleotide diversity ($\pi \pm$ SD) of 0.0031 ± 0.0003. Their phylogenetic relationships appeared as a star-like topology with a central dominant haplotype, from which several low-frequency haplotypes radiate and diverge just by one or a few mutations (*SI Appendix*, Fig. S1). Standard neutrality tests and mismatch distribution identified a population expansion signature, with significant negative values for Tajima's D (−2.22; $P < 0.01$) and Fu's Fs (−35.8; $P < 0.0001$) statistics and a clearly unimodal mismatch distribution (*SI Appendix*, Fig. S2).

Genetic Variation at the Autosomal Microsatellite Loci. The genetic diversity at the 10 nuclear autosomal microsatellite loci is described in Table 1. The overall allelic richness value was 6.9 (minimum = 1.9 and maximum = 10.9); the observed and expected heterozygosity were H_o = 0.50 (minimum = 0.01 and maximum = 0.77) and H_e = 0.49 (minimum = 0.01 and maximum = 0.75), respectively; and the fixation index (F_{IS}) value was −0.033, not significantly different from 0 (permutation test, $P = 0.982$), indicating no significant departure from Hardy–Weinberg expectations (Table 1). The mean ratio between the number of alleles and the range in allele sizes [Garza and Williamson's index (M_{GW})] at microsatellite loci can be used to detect population size changes (33). The value that we observed (M_{GW} = 0.635) was typical of a declining population (33), in contrast to the mtDNA results.

Panmictic Population in the Black Sea and Aegean Sea. Previous studies suggested that population subdivision might exist between harbor porpoises from the Aegean Sea and the Black Sea (28, 29). However, we did not detect any significant differences in the mtDNA-CR haplotypic frequencies between porpoises

Table 1. Genetic diversity and fixation indices at the 10 microsatellite loci for harbor porpoises from the Black Sea and Aegean Sea

Locus	*n*	A_r	H_o/H_e	F_{IS}
415–416	76	4.0	0.38/0.44	0.129
EV94	88	4.0	0.48/0.48	−0.017
GATA53	89	1.9	0.01/0.01	0.000
GT11	88	3.9	0.44/0.39	−0.110
GT15	86	10.9	0.39/0.37	−0.057
Ig-F1	89	10.9	0.77/0.75	−0.034
PPH104	86	9.0	0.70/0.65	−0.065
PPH110	85	6.0	0.53/0.50	−0.065
PPH130	89	7.9	0.63/0.65	0.029
PPH137	87	9.9	0.70/0.64	−0.099
Multilocus	86	6.9	0.50/0.49	−0.033

A_r, allelic richness; F_{IS}, departure from panmixia; H_e, gene diversity; H_o, observed heterozygosity; *n*, sample size.

from the Aegean Sea and the Black Sea, neither at the haplotypic level (fixation index F_{ST} = 0.05, χ^2 = 27.2, P = 0.66, df = 31) nor at the nucleotide level (Hudson's nearest neighbor distance Snn = 0.75, P = 0.281). Half of the animals from the Aegean Sea carried the dominant haplotypes, and only 3 of the 10 individuals from the Aegean Sea each carried a unique mtDNA haplotype (*SI Appendix*, Fig. S1 and Table S1).

Similarly, we did not observe any private allele at the microsatellite loci in the Aegean Sea porpoises and no significant differences in allelic frequencies between Aegean Sea and Black Sea porpoises [F_{ST} = 0.016, 95% confidence interval (CI): (0–0.035), P = 0.119]. We further tested the occurrence of population subdivision using the Bayesian model-based clustering analysis implemented in STRUCTURE v2.3.3 (34). The two admixture models tested, namely, the standard model and the "*locprior*" model designed to detect weak population structure (34), both revealed no evidence for population subdivision (*SI Appendix*, Fig. S3). Harbor porpoises from the Black Sea and the Aegean Sea thus form a single random-mating population.

Detection and Quantification of Population Size Change. We compared 15 scenarios of demographic changes in the Black Sea population, which differed in the type of changes in population size considered (i.e., stability, expansion, collapse, bottleneck, expansion-decline) and in the timing of these changes (i.e., a recent change within the past 100 generations vs. an ancient change between 100 and 1,000 generations) (*Materials and Methods*, Fig. 2, and *SI Appendix*, Table S2). We analyzed 1.5 million simulated datasets generated for each scenario (i.e., a total of 22.5 million datasets) using the ABC framework of DIY-ABC v1.0.4.46b program (35).

We first evaluated the relative posterior probability of each competing scenario using a polychotomous logistic regression (35, 36) on the 1% of simulated datasets closest to the observed dataset (Table 2). These posterior probabilities unambiguously pointed to the group of scenarios (SC14 and SC15; Fig. 2) that assumed an ancient expansion from a small ancestral population (with a size N_{1lc}) that reached a large effective population size (N_a) and then went through a severe population reduction within the past 100 generations to reach its current size (N_1). This group of scenarios was selected with a very high posterior probability ($P > 0.999$) relative to the 13 others. In the 2 scenarios within this group, scenario SC15, which differed from SC14 by allowing the current population size (N_1) to be distinct from the one at the time of the foundation (N_{1lc}), received significantly greater support than scenario SC14, with a posterior probability of 0.57 [95% CI: (0.56–0.59)] and 0.42 [95% CI: (0.41–0.44)], respectively.

We next evaluated the power of the model choice procedure using the method implemented in DIY-ABC (Table 2), following the recommendations of Robert et al. (37). For that purpose, we first simulated 500 random datasets under the selected scenario (SC15) and computed the proportion of cases in which this scenario did not display the highest posterior probability among all scenarios. This empirical estimate of the type I error was only 12.4%. We then empirically estimated the type II error rate by simulating 100 random datasets under each alternative scenario (SC1 to SC13, excluding SC14 because it is nested within SC15) and computing the proportion of cases in which SC15 was incorrectly selected as the most likely scenario on these simulated datasets (Table 2). The average type II error rate was only 6.7%, indicating a 93.3% statistical power. Hence, this simulation-based evaluation of the performance of the ABC model choice procedure (37) clearly showed that, given the size and polymorphism of our dataset, the method had high power to distinguish between the alternative demographic scenarios that we investigated.

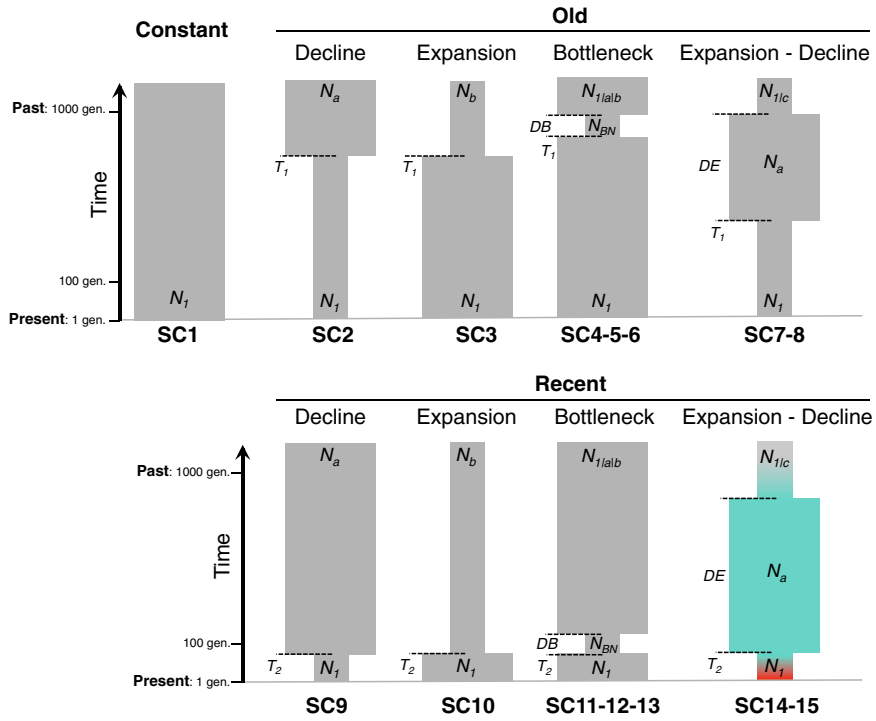

Fig. 2. Alternative scenarios of harbor porpoise evolution in the Black Sea tested using the ABC approach. The colored scenario SC14–SC15 was the one displaying the highest posterior probabilities (Table 2). It embedded two nested scenarios: SC14, which assumed that an ancestral population increased in size and decreased back to the same initial size, and SC15, which allowed for distinct initial and final population sizes. Details of each scenario parametrization are provided in *Materials and Methods* and in *SI Appendix*, Table S2. The time scale is indicated by the arrow on the left. Time was measured backward in generations before the present. gen, generation.

Table 2. Model choice and performance analyses of the ABC analysis

Scenario	Post. prob. (95% CI)	P(SC15)*	Outlying summary statistics† $P < 0.05$	$P < 0.01$	$P < 0.001$
SC1	0%	0.12‡	3	0	2
SC2	0%	0.01‡	3	1	1
SC3	0%	0.10‡	3	1	1
SC4	0%	0.11‡	0	1	1
SC5	0%	0.03‡	0	1	1
SC6	0%	0.03‡	3	1	1
SC7	0%	0.20‡	3	1	1
SC8	0%	0.12‡	3	1	1
SC9	0%	0.07‡	3	1	1
SC10	0%	0.00‡	2	3	2
SC11	0%	0.03‡	0	1	1
SC12	0%	0.04‡	3	1	1
SC13	0%	0.01‡	2	2	3
SC14	42.4% (40.8–44.0)	—	1	1	0
SC15	57.6% (56.0–59.2)	0.88§	2	0	0

Post. prob., relative posterior probability for each competing scenario.
*P(SC15) is the proportion of pseudoobserved datasets simulated using each competing scenario (SC1 to SC13 and SC15) for which SC15 was selected because it displayed the highest posterior probability with nonoverlapping confidence intervals.
†Number of summary statistics used to discriminate among the competing scenarios that displayed outlying values compared with the observed ones. Details on the *P* value calculation are provided in *Materials and Methods* and *SI Appendix*, Table S3. Individual *P* values reported for each summary statistic and each competing scenario are provided in *SI Appendix*, Table S3.
‡For SC1 to SC13, P(SC15) represents an empirical estimate of the model specific type II error rate.
§For SC15, 1 − P(SC15) provides an empirical estimate of the type I error rate (here, 12%).

We estimated the marginal posterior probability density for each parameter of the expansion-decline scenario (SC15) using the 1% closest simulated datasets from the observed dataset (i.e., 15,000 datasets; *Materials and Methods*) (parameters in demographic units are provided in Table 3 and Fig. 3; parameters scaled by the mutation rate are provided in *SI Appendix*, Figs. S4 and S5). Under this model, we estimated that a small population with an effective size of ∼299 individuals [90% highest probability density interval (HPDI): (41–872)] colonized the Black Sea and expanded to an effective population size of 7,500 individuals [90% HPDI: (3,500–16,154); i.e., a 15-fold factor [90% HPDI: (4–72)]. We estimated that this expansion occurred 1,499 [90% HPDI: (1,007–4,897)] years before present (ybp). This estimated time was based on a generation time of 10 y, as recommended by Birkun and Frantzis (15). Regarding the recent population decline, we estimated that during the past 5 decades [90% HPDI: (5–48) ybp], the population of Black Sea harbor porpoises was reduced to only 10% [90% HPDI: (3–16%)] of its former size. The current effective population size was indeed estimated to be around 700 individuals [95% CI: (222–1,619)]. This value is highly consistent with an independent estimate of 708 for the current effective population size obtained from the linkage disequilibrium pattern between microsatellite loci using the program LDNe (38).

Table 3. Demographic parameters estimated under the best-supported demographic scenario (SC15) of an "old" ancestral expansion and a recent population decline

Parameter	Mode*	90% HPD†
Current effective population size (N_1)‡	699	222–1,619
Population size before the collapse (N_a)‡	7,518	3,464–16,154
Population size at the foundation (N_c)‡	299	41–872
Magnitude of the population decline (N_1/N_a)	0.10	0.03–0.16
Magnitude of the population expansion (N_a/N_c)	15.1	3.6–71.8
Time since the expansion (T_2 + DE), ybp§	1,499	1,007–4,897
Time since the decline (T_2), ybp§	9	5–48

*Modal value of the marginal posterior probability density.
†Lower and higher bounds of the 90% HPDI.
‡Population sizes are given in effective number of diploid individuals.
§Time estimates were calibrated by assuming a generation time of 10 y as recommended by Birkun and Frantzis (15).

Finally, to assess the goodness-of-fit of the estimated model to the data, we simulated 1,000 datasets under each scenario tested, drawing the values of their parameters into the marginal posterior distributions of these parameters. We thus identified which model was the most capable of reproducing the observed summary statistics computed from the real data, following the model-checking procedure described by Cornuet et al. (35). Compared with the 13 other demographic scenarios tested, only the datasets simulated under the expansion-decline scenario (SC15, and SC14 to a lesser extent) were compatible with the observed summary statistics computed from the real data. This can be observed by comparing the values of summary statistics computed from simulated datasets for each tested scenario against the real values (Table 2 and *SI Appendix*, Fig. S6 and Table S3). With the exception of SC15 (and SC14 to a lesser extent), all competing scenarios generated large numbers of summary statistics that displayed highly significant outlying values. This finding hence provides further support to the very high posterior probability values obtained for SC15 and SC14 using the model choice procedure (see above).

Discussion

Our study shows that the present-day genetic diversity of Black Sea harbor porpoises has been strongly influenced by an initial founder event that took place several thousand years ago, followed by a dramatic decrease in population size within the past 5 decades. Such clear signals of recent population decline in genetic data have only rarely been documented previously [e.g., the collapse of orangutan populations in Sumatra and Borneo (39)]. However, our study reports both a recent event of decline and an ancient event of expansion from contemporary genetic data, showing the great power of coalescent-based analyses, especially in the flexible framework provided by ABC methods.

Mitochondrial and nuclear autosomal microsatellite loci were informative at different time scales, highlighting different episodes in the demographic history of Black Sea harbor porpoises. The structure of mtDNA-CR genetic diversity reflected the demographic expansion that occurred after the foundation of the population in the Black Sea, once it was reconnected to the Mediterranean Sea around 8,000 ybp (40). Conversely, the microsatellite data were more informative on contemporary demography (i.e., current population declines). Such a difference in demographic signals captured by each type of genetic marker can arise from the differences in their respective mutation rates (discussion of some simulation-based testing is included in ref. 35). The relatively fast mutation rate of microsatellite loci enables them to capture recent and almost contemporaneous events but also increases homoplasy at these loci, which thereby reduces the signal of older demographic events (41). These more ancient events can, however, still be detected using the slower evolving mtDNA sequences.

Selective processes, instead of demographic processes (genetic drift), could be proposed as an alternative explanation for the observed pattern of genetic diversity at microsatellite and mitochondrial loci. However, this is very unlikely for several reasons. Demographic processes usually affect the entire genome, whereas

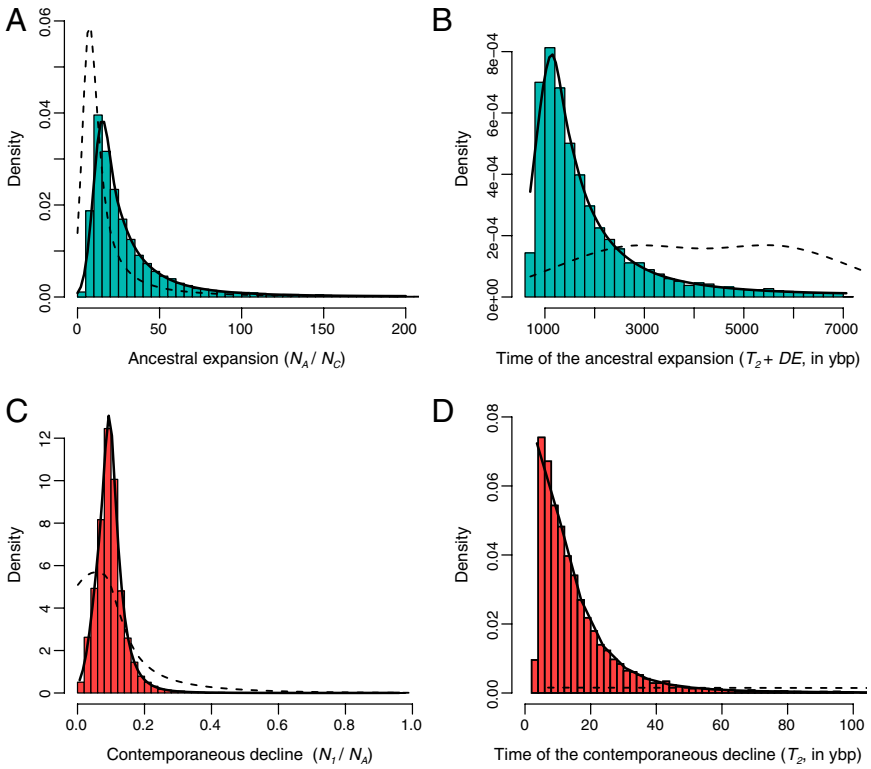

Fig. 3. Marginal posterior probability densities (solid lines and histograms) for the intensity of the ancestral expansion (*A*) and its timing (*B*) and the contemporaneous decline (*C*) and its timing (*D*), obtained from the DIY-ABC analysis under the best-supported demographic scenario (SC15) of an "old" ancestral expansion and a recent population decline (details on this scenario are provided in Fig. 2 and *SI Appendix*, Table S2). The dotted lines show the prior distributions for each parameter.

selective processes usually target specific loci in the genome (42). Because we studied 10 independent microsatellite loci, we can rule out the possibility that selection is the main force shaping their genetic diversity, because it would target one or a few of them but not all (42). Moreover, in any species, genetic diversity results from a balance between genetic drift and selective processes, with the relative contribution of these two forces depending on population size (42). In large mammals, and particularly in endangered species, the low effective population size leaves little room for selective processes to act, and genetic drift is thus the principal force shaping genetic diversity (23, 42). This argument applies even more to the mitochondrial genome, for which haploid nature and maternal inheritance make the effective population size four times smaller than that of any autosomal loci in the nuclear genome. The very small effective population size of the Black Sea harbor porpoises should thus make selective forces very inefficient in comparison to genetic drift (42, 43). It is therefore very unlikely that the mitochondrial diversity patterns observed here result from a selective sweep. Finally, the strong concordance between our demogenetic inferences, the historical records, and the biogeography of the Black Sea basin argues against selective processes as a putative explanation and, instead, supports the influence of demographic events.

Indeed, our ABC study allowed us to make strong quantitative inferences about the demographic history of the harbor porpoise in the Black Sea. First, we estimated that a few hundred individuals took refuge in the Black Sea when environmental conditions for this species became unsuitable in the Mediterranean Sea. The low estimate of the effective size of this founder population (N_e = 300) suggests that only a few individuals managed to cross the newly opened Bosporus and Dardanelles straits into the Black sea. Second, we showed that this population subsequently underwent a drastic 15-fold expansion. The point estimate from this expansion time was ~1,500 ybp, and the 90% HPDI suggested that this event took place within the past 5,000 ybp. These estimates are quite consistent with a previous population genetics study that showed the split between the harbor porpoise populations from the Black Sea and the Atlantic waters most likely occurred within the past 6,000 ybp (27). The discrepancy between the reconnection of the Black Sea to the Mediterranean Sea (8,000 y ago) and the maximum value that we estimated for the expansion time of the porpoise population (5,000 y ago) might simply result from a lack of accuracy in the genetic estimation of the time or of the mutation rate (27). On the other hand, it is reasonable to argue that some time was required, after the Black Sea was reconnected to the Mediterranean Sea, to restore marine conditions fully in this previously hyposaline body of water, and thereby to create suitable habitat conditions for harbor porpoise settlement and expansion (40).

Regarding the recent history of this subspecies, we were able to infer that it underwent a very drastic reduction in population size. This finding can be clearly related to the massive mortality of small cetaceans in the commercial hunt, which continued until 1983 and severely reduced the population size of harbor porpoises (44, 45). However, little information is available on the census number of individuals that existed before the start of the dolphin fisheries activities and on the census size of porpoises currently inhabiting the Black Sea. The current census size may be at least several thousand, and possibly in the low tens of thousands of individuals (15). On the other hand, we estimated a substantially lower effective population size of around 700 individuals. These two estimates are not necessarily incompatible because they are not expected to have the same magnitude in natural populations (23, 46). The census population size estimated from field

surveys accounts for all living individuals (calves, subadults, and breeding and nonbreeding adults), whereas the effective sample size is a theoretical concept in population genetics, which refers to the number of individuals in an ideal population (Wright–Fisher model) that would have the same genetic diversity as the one observed in the population (42). The effective population size thus depends on social structure, the number of breeding individuals, and the demographic history among other factors and is usually substantially smaller than the census size (23, 47).

However, the ratio between the estimated effective population sizes before and after dolphin fisheries provides a rather accurate indication of the changes in census population sizes and offers the additional advantage of being independent of any mutation rate estimates. Using historical records, it was suggested that harbor porpoise population was reduced to at least 70% of its size before hunting activities (15, 48). Based solely on contemporary genetic data, we find a reduction of 90% [90% HPDI: (84–97%)], which suggests an even stronger population decline in the past 50 y. It is remarkable to note the strong concordance between the estimates drawn from genetic data and from fisheries records. Interestingly, ecosystem modeling studies also suggested that a 10-fold reduction of dolphin and porpoise populations could account for the observed trophic cascades that triggered regime shifts in the Black Sea (11). Our genetic inference on the magnitude of the population decline is thus highly consistent with the value predicted from ecosystem modeling.

Although dolphin fisheries were banned in the countries surrounding the Black Sea, populations of small cetaceans are unlikely to have recovered much since 1983. Incidental catches in commercial fisheries are still having a severe impact on small cetacean populations in the Black Sea, particularly on harbor porpoises, which are the predominant species in the by-catch of fisheries nowadays, killing thousands of animals each year (15). Accordingly, demographic scenarios of bottlenecks followed by a recent expansion were highly incompatible with the observed genetic data. On the other hand, genetic signals of population recovery would probably not become instantly visible but may require some time (20). Nonetheless, our study lends support to the theory that the dolphin fishery caused a strong abundance decline in Black Sea harbor porpoises, from which they have not yet started to recover but, instead, continue to decline, primarily due to large-scale mortality in bottom-set gillnets and habitat degradation (15).

Conclusions

The Black Sea is an exceptional natural laboratory for which the impact of predator release on the structure and dynamics of the trophic network has been deeply and intensively studied (7, 8, 11). However, quantifying the extent to which top predators were actually decimated to trigger such an ecosystem-wide effect is particularly challenging because of the scarcity and biased nature of the information provided by historical records. Population genetics can provide relevant information in this context. In particular, the isolated status of Black Sea harbor porpoises made this population well suited to study demographic changes from a genetic perspective, avoiding the risk of confounding factors, such as external gene flow. It allowed us to provide an independent assessment of the impact of large-scale fisheries-induced mortality on the demography of a top marine predator in the Black Sea.

Current demographic declines in endangered species are usually confounded by historical events (23, 39). Our ABC approach, which relied on large-scale computer simulations, provided the flexible statistical framework required to compare alternative demographic scenarios. Using genetic markers evolving at different rates, we were able to capture and separate the effects of recent anthropogenic collapse related to dolphin hunting practices and the ancient population expansion related to the postglacial foundation of this population. Moreover, we could estimate the effective size of the founding population and its establishment time, two parameters that could not be estimated by any other means. Inferring two successive demographic events from genetic data underlines the great power and flexibility of ABC approaches, which are still to be applied more widely in conservation biology (31). This study thus demonstrates how population genetics approaches can provide valuable additional information to historical and ecological modeling studies.

Materials and Methods

Sample and DNA Extraction. Skin and muscle samples were collected from 89 harbor porpoises stranded along the coasts of the Black Sea (n = 75), Marmara Sea (n = 3), and Aegean Sea (n = 11) (Fig. 1). Total genomic DNA was extracted from tissue samples using a PureGene and DNeasy Tissue kit (Qiagen), following the manufacturer's recommendations.

Mitochondrial Data and Analyses. The complete MtDNA-CR was amplified as described by Fontaine et al. (27). Sequences were automatically aligned using the Clustal W algorithm implemented in Bioedit 7.0.9 (49) and checked visually afterward. A median-joining network was generated to infer phylogenetic relationships among the mtDNA haplotypes using the program NETWORK v4.6 (www.fluxus-engineering.com) (50). MtDNA-CR haplotypic (H_d) and nucleotidic (π) diversities, Tajima's D (51) and Fu's Fs (52) statistics, and mismatch distribution were computed using DnaSP V5.10 (53). The differences between porpoises from the Aegean Sea and the Black Sea were tested both at the haplotypic level using Weir and Cockerham's (54) estimator of F_{ST} (55) and at the nucleotide level using the Snn statistic (56). The statistical significance of the difference in haplotypic frequencies was tested by means of a permutation test (10^5 permutations) using DnaSP v5.10 (53).

Microsatellite Data and Analyses. Genotypes at 10 microsatellite loci from the same 78 porpoises from the Black Sea were taken from the study by Fontaine et al. (24), to which we added 11 newly genotyped porpoises from the Aegean Sea (Fig. 1), following the genotyping procedure described by Fontaine et al. (24, 57). Genetic polymorphism at each locus was quantified using the allelic richness (A_r), the observed and unbiased expected heterozygosity (H_o and H_e), and the fixation index (F_{IS}). These statistics were calculated using FSTAT 2.9.3.2 (58). Departure from Hardy–Weinberg expectations was tested using exact tests implemented in GENEPOP 4.0 (59, 60). Linkage disequilibrium among loci was tested using a permutation test (10^5 permutations) implemented in FSTAT 2.9.3.2 (58). The nominal P value of 0.05 was adjusted for multiple comparisons using a Bonferroni correction. Differences in allelic frequencies between porpoises from the Aegean Sea and the Black Sea were tested using the exact tests implemented in GENEPOP 4.0 and quantified using the Weir and Cockerham estimator of F_{ST} (54).

Bayesian Clustering Methods. We further investigated the population structure using the Bayesian method of individual clustering implemented in STRUCTURE v2.3.3 (34, 61, 62). This analysis partitions multilocus genotypes into clusters, while minimizing departure from Hardy–Weinberg expectations and linkage equilibrium among loci, and it estimates individual ancestry proportions to each putative cluster. We conducted the analyses on the multilocus microsatellite dataset to which we added the individual mtDNA haplotypes, recoded following the STRUCTURE program's user guide. The analysis was performed using the "standard" model of admixture and allele frequencies correlated among populations, as well as the recently developed "*locprior*" model designed to detect weak population structure by making explicit use of sampling location information (34). For this purpose, we introduced the a priori assumption that porpoises from the Black Sea and the Aegean Sea were coming from two distinct populations, by modifying the prior on individual origin in the model (34). We conducted a series of independent runs with different assumed values for the number of clusters (K), testing all values from 1 to 5. Each run used 500,000 iterations after a burn-in of 50,000 iterations. To ensure convergence of the Markov chain Monte Carlo, we performed 10 independent replicates for each value of K. The number of clusters that best explains the data was assessed by computing the posterior probability, $P(X|K)$, of the data for a given number of assumed clusters and by computing the rate of change of this value as K increased (63).

Detection and Quantification of Population Size Change. We inferred the demographic history of harbor porpoise from the Black Sea and Aegean Sea using the ABC approach (30, 32) implemented in the computer program DIY-ABC v1.0.4.46b (35). This approach allows choice of the demographic scenario that

best fits the data and inference of the posterior probability distributions for the parameters of interest under this preferred scenario. The different steps of the ABC parameter estimation procedure are described in detail elsewhere (31, 32, 64), but we briefly outline them below.

Tested evolutionary scenarios. We compared 15 demographic scenarios, which are graphically depicted in Fig. 2. SC1 consists of a null hypothesis assuming a population whose effective size (N_1) remained stable over time. SC2 assumed that a population of size N_a declined instantaneously to its current effective size (N_1) T generations ago. Conversely, SC3 assumed that a population of effective size N_b increased instantaneously T generations ago to reach its current effective size (N_1). SC4 to SC6 assumed a bottleneck event, where the population, with an initial effective size of $N_{1|a|b}$, decreased to a lower size (N_{BN}) at which it remained for a short period (DB), and then recovered back to a larger current population size (N_1). The three bottleneck scenarios differed from each other in the initial and final population sizes (SC4: $N_1 = N$, SC5: $N_1 < N_a$, and SC6: $N_1 > N_b$). The final class of models (SC7 and SC8) assumed the reverse situation, where a population of small size ($N_{1|c}$) increased instantaneously $T + DE$ generations ago to reach the size N_a, and declined to reach its current size (N_1) T generations later. SC7 and SC8 differed from each other in the initial and final population sizes. In SC7, the initial population size was forced to be equal to the final population size, whereas in SC8, the two could be distinct. For scenarios SC2 to SC8, we considered two plausible ranges of time, T, during which these events could have occurred (i.e., T_1 = 100–1,000 generations and T_2 = 1–100 generations; *SI Appendix*, Table S2). We did so to test whether these changes in effective population size were more compatible with an old event related to the postglacial founder event of the Black Sea or with a recent event related to the recent anthropogenic perturbations in the Black Sea. Scenarios SC2 to SC8 therefore refer to events that could have occurred between 100 and 1,000 generations ago, and scenarios SC9 to SC15 refer to more recent events between 1 and 100 generations ago (Fig. 2).

ABCs. For each of the 15 models, we simulated 1.5 million datasets based on a demographic history that describes the model, using the program DIY-ABC. Some or all parameters that define each model (i.e., population sizes, timing of the demographic events, mutation rates) were considered as random variables for which some prior distribution must be defined, as shown in *SI Appendix*, Table S2. For each simulation, the parameter values are drawn from their prior distributions, defining a demographic history that is used to build a specific input file for the DIY-ABC program. DIY-ABC then performs coalescent-based simulations to generate the genetic diversity of samples, with the same number of gene copies and loci as those observed. It then computes, for the simulated datasets, the summary statistics (S), which were also computed on the observed data (S*). Following the method of Storz and Beaumont (21), a Euclidean distance, δ, was calculated between normalized S and S* for each simulated dataset.

Mutation model. The coalescent simulations require a mutation model to be defined for each type of marker used. Here, we jointly analyzed the mtDNA-CR and microsatellite data. The mutation model that best described the sequence evolution of the mtDNA-CR was a Hasegawa–Kishino–Yano mutation model (65) as recommended by Palsbøll et al. (66), assuming a per-site and generation mutation rate ranging uniformly between 1×10^{-7} and 1×10^{-5} mutations, a proportion of constant sites of 82%, and a shape of the gamma distribution of mutations among sites equal to 0.9 (*SI Appendix*, Table S2). These two latter values were empirically determined from the observed data using jModelTest 0.1.1 (67).

The 10 microsatellite loci were assumed to follow a generalized stepwise mutation model (41) with two parameters: the mean mutation rate (μ) and the mean parameter of the geometrical distribution assumed for the length in repeat numbers of mutation events (P) drawn from Uniform (10^{-5} to 10^{-3}) and Uniform (0.1–0.3) prior distributions, respectively. Each locus has a possible range of 40 contiguous allelic states and was characterized by individual μ_{loc} and P_{loc} values, drawn from gamma distributions with respective means μ and P and shape parameter 2 in both cases (68). Using this setting, we allowed for large mutation rate variance across loci (i.e., range of 10^{-5} to 10^{-2}). We also considered mutations that insert or delete a single nucleotide to the microsatellite sequence. We used default values for any other mutation model settings. Details on model parameterization and prior settings are supplied in *SI Appendix*, Table S2.

Summary statistics. Summary statistics of genetic diversity were calculated with DIY-ABC. The following statistics were computed for microsatellite loci: mean number of alleles per locus (A), mean expected heterozygosity (H_e), mean allele size variance (V), and mean M_{GW} index across loci (33). The descriptive statistics computed to describe the variation at the mtDNA-CR were the number of haplotypes (NHA), the number of segregating sites (NSS), the mean pairwise differences (MPD) and its variance (VPD), and Tajima's D statistics.

Model choice procedure and performance analyses. The posterior probability of each competing scenario was estimated using a polychotomous logistic regression (35, 36) on the 1% of simulated datasets closest to the observed dataset. We evaluated the ability of our ABC methodology to discriminate between scenarios by analyzing simulated datasets with the same number of loci and individuals as in our real dataset. Following the method of Cornuet et al. (35), we estimated the type I error probability as the proportion of instances where the selected scenario did not exhibit the highest posterior probability compared with the competing scenarios for 500 simulated datasets generated under the best-supported model (SC15). In a similar way, we estimated the type II probability by simulating 100 datasets for each of 13 alternative scenarios (with SC14 being excluded because it is a similar model nested within SC15) and calculating the mean proportion of instances in which the best-supported model was incorrectly selected as the most probable model.

Parameter estimation and goodness of fit. We estimated the posterior distributions of demographic parameters under the best demographic model, using a local linear regression on the 1% closest of 1.5×10^6 simulated datasets, after the application of a *logit* transformation to parameter values (30, 36). Finally, following the method of Gelman et al. (69), we evaluated whether under the best model-posterior combination, we were able to reproduce the observed data using the model checking procedure available in DIY-ABC v.1.0.4.46b (35). Model checking computations were processed by simulating 1,000 pseudoobserved datasets under each studied model-posterior combination, with sets of parameter values drawn with replacement among the 1,000 sets of the posterior sample. This generated a posterior cumulative distribution function for each summary statistic, allowing us to estimate the P values for the observed values of these summary statistics. In addition, a principal component analysis (PCA) was performed in the space of summary statistics. Principal components were computed considering 15,000 datasets simulated with parameter values draw from the prior. The target (observed) dataset, as well as the 1,000 datasets simulated from the posterior distributions of parameters, was then added to each plane of the PCA.

ACKNOWLEDGMENTS. We thank all the fishermen, stranding networks, and volunteers who contributed to the collection of samples used in the present study, particularly A. Birkun, Jr. (ACCOBAMS and BREMA laboratory, Ukraine). We also thank M. A. Beaumont, A. E. Estoup, and F. P. Palstra for their advice and discussions on the ABC procedures. We acknowledge F. P. Palstra, K. A. Tolley, S. J. E. Baird, three anonymous reviewers, and the editor for comments on the manuscript and English editing. ABC estimations were performed at the cluster computation facilities at the National Museum for Natural History (Paris). We thank Julio Pedraza Acosta for his assistance in the use of this cluster. This work was partly funded by the Belgian Science Policy under Project VIPHOGEN-SSTC EV/12/46A.

1. Aristotle (2001) *Historia Animalium* (Univ of Virginia Press, Charlottesville, VA), Vol 4, Book 8. Available at http://etext.virginia.edu/toc/modeng/public/AriHian.html. Accessed November 26, 2011.
2. Zaitsev Y (1993) Impact of eutrophication on the Black Sea fauna. *Studies and Reviews, Fisheries and Environment Studies in the Black Sea System* (General Fisheries Council for the Mediterranean, Food and Agriculture Organization of the United Nations, Rome), Vol 64, pp 59–86.
3. Bologa A, Bodeanu N, Petran A, Tiganus V, Zaitzev Y (1995) Major modifications of the Black Sea benthic and planktonic biota in the last three decades. *Bulletin de l'Institut Océanographique* 1:85–110.
4. Daskalov GM (2003) Long-term changes in fish abundance and environmental indices in the Black Sea. *Mar Ecol Prog Ser* 255:259–270.
5. Oguz T, Dippner JW, Kaymaz Z (2006) Climatic regulation of the Black Sea hydrometeorological and ecological properties at interannual-to-decadal time scales. *J Mar Syst* 60:235–254.
6. Bilio M, Niermann U (2004) Is the comb jelly really to blame for it all? *Mnemiopsis leidyi* and the ecological concerns about the Caspian Sea. *Mar Ecol Prog Ser* 269: 173–183.
7. Llope M, et al. (2011) Overfishing of top predators eroded the resilience of the Black Sea system regardless of the climate and anthropogenic conditions. *Glob Change Biol* 17:1251–1265.
8. Daskalov GM, Grishin AN, Rodionov S, Mihneva V (2007) Trophic cascades triggered by overfishing reveal possible mechanisms of ecosystem regime shifts. *Proc Natl Acad Sci USA* 104:10518–10523.
9. Mee L, Friedrich J, Gomoiu MT (2005) Restoring the Black Sea in times of uncertainty. *Oceanography (Wash D C)* 18:100–111.
10. Oguz T, Gilbert D (2007) Abrupt transitions of the top-down controlled Black Sea pelagic ecosystem during 1960–2000: Evidence for regime-shifts under strong fishery exploitation and nutrient enrichment modulated by climate-induced variations. *Deep-Sea Res,* Part I 54:220–242.

11. Daskalov GM (2002) Overfishing drives a trophic cascade in the Black Sea. *Mar Ecol Prog Ser* 225:53–63.
12. Kleinenberg SE (1956) *Mammals of the Black and Azov Seas: Research Experience for Biology and Hunting* (USSR Academy of Science Publishing House, Moscow).
13. Geptner VG, Chapsky KK, Arsenyev VA, Sokolov VE (1976) *Mammals of the Soviet Union. Pinnipeds and Toothed Whales* (Vysshaya Shkola, Moscow), Vol 2, Part 3.
14. Jefferson TA, Leatherwood S, Webber MA (1993) *FAO Species identification Guide. Marine Mammals of the World* (UNEP/FAO, Rome).
15. Birkun AA, Jr., Frantzis A (2008) Phocoena phocoena ssp. relicta. IUCN Red List of Threatened Species. Version 2011.1, Available at www.iucnredlist.org. Accessed September 5, 2011.
16. Berkes F (1977) Turkish dolphin fisheries. *Oryx* 14:163–167.
17. Alter SE, Rynes E, Palumbi SR (2007) DNA evidence for historic population size and past ecosystem impacts of gray whales. *Proc Natl Acad Sci USA* 104:15162–15167.
18. Roman JR, Palumbi SR (2003) Whales before whaling in the North Atlantic. *Science* 301:508–510.
19. Lawton-Rauh A (2008) Demographic processes shaping genetic variation. *Curr Opin Plant Biol* 11(2):103–109.
20. Girod C, Vitalis R, Leblois R, Fréville H (2011) Inferring population decline and expansion from microsatellite data: A simulation-based evaluation of the Msvar method. *Genetics* 188:165–179.
21. Storz JF, Beaumont MA (2002) Testing for genetic evidence of population expansion and contraction: An empirical analysis of microsatellite DNA variation using a hierarchical Bayesian model. *Evolution* 56:154–166.
22. Beaumont MA (1999) Detecting population expansion and decline using microsatellites. *Genetics* 153:2013–2029.
23. Frankham R, Ballou JD, Briscoe DA (2002) *Introduction to Conservation Genetics* (Cambridge Univ Press, Cambridge, UK).
24. Fontaine MC, et al. (2007) Rise of oceanographic barriers in continuous populations of a cetacean: The genetic structure of harbour porpoises in Old World waters. *BMC Biol* 5:30.
25. Rosel P, Dizon AE, Haygood MG (1995) Variability of the mitochondrial control region in populations of the harbour porpoise, *Phocoena phocoena*, on interoceanic and regional scales. *Can J Fish Aquat Sci* 52:1210–1219.
26. Frantzis A, Gordon J, Hassidis G, Komenou A (2001) The enigma of harbour porpoise presence in the Mediterranean Sea. *Mar Mamm Sci* 17:937–943.
27. Fontaine MC, et al. (2010) Genetic and historic evidence for climate-driven population fragmentation in a top cetacean predator: The harbour porpoises in European waters. *Proc Biol Sci* 277:2829–2837.
28. Rosel PE, Frantzis A, Lockyer C, Komnenou A (2003) Source of Aegean sea harbour porpoises. *Mar Ecol Prog Ser* 247:257–261.
29. Viaud-Martinez KA, et al. (2007) Morphological and genetic differentiation of the Black Sea harbour porpoise *Phocoena phocoena*. *Mar Ecol Prog Ser* 338:281–294.
30. Beaumont MA, Zhang W, Balding DJ (2002) Approximate Bayesian computation in population genetics. *Genetics* 162:2025–2035.
31. Bertorelle G, Benazzo A, Mona S (2010) ABC as a flexible framework to estimate demography over space and time: some cons, many pros. *Mol Ecol* 19:2609–2625.
32. Csilléry K, Blum MGB, Gaggiotti OE, François O (2010) Approximate Bayesian Computation (ABC) in practice. *Trends Ecol Evol* 25:410–418.
33. Garza JC, Williamson EG (2001) Detection of reduction in population size using data from microsatellite loci. *Mol Ecol* 10:305–318.
34. Hubisz MJ, Falush D, Stephens M, Pritchard JK (2009) Inferring weak population structure with the assistance of sample group information. *Mol Ecol Resour* 9: 1322–1332.
35. Cornuet JM, Ravigné V, Estoup A (2010) Inference on population history and model checking using DNA sequence and microsatellite data with the software DIYABC (v1.0). *BMC Bioinformatics* 11:401.
36. Cornuet JM, et al. (2008) Inferring population history with DIY ABC: A user-friendly approach to approximate Bayesian computation. *Bioinformatics* 24:2713–2719.
37. Robert CP, Cornuet JM, Marin JM, Pillai NS (2011) Lack of confidence in approximate Bayesian computation model choice. *Proc Natl Acad Sci USA* 108:15112–15117.
38. Waples RS, Do CHI (2008) ldne: A program for estimating effective population size from data on linkage disequilibrium. *Mol Ecol Resour* 8:753–756.
39. Goossens B, et al. (2006) Genetic signature of anthropogenic population collapse in orangutans. *PLoS Biol* 4(2):e25.
40. Rohling EJ, Abu-Zieb R, Casford JLS, Hayes A, Hoogakker BAA (2009) The marine environment: Present and past. *The Physical Geography of the Mediterranean*, ed Woodward JC (Oxford Univ Press, Oxford), pp 33–67.
41. Estoup A, Jarne P, Cornuet JM (2002) Homoplasy and mutation model at microsatellite loci and their consequences for population genetics analysis. *Mol Ecol* 11:1591–1604.
42. Hartl DL, Clark AG (2007) *Principle of Population Genetics* (Sinauer Associates, Sunderland, MA), 4th Ed.
43. Mulligan CJ, Kitchen A, Miyamoto MM (2006) Comment on "Population size does not influence mitochondrial genetic diversity in animals.". *Science* 314:1390.
44. Smith TD (1982) Current understanding of the status of the harbour porpoise populations in the Black Sea. Mammals in the Seas, Vol. 4. *Food and Agriculure Organization of the United Nations Fisheries Series* 5:121–130.
45. IWC (2004) Annex L. Report of the Sub-committee on Small Cetaceans. *J Cetacean Res Manag* 6:315–334.
46. Waples RS, Gaggiotti OE (2006) What is a population: An empirical evaluation of some genetic methods for identifying the number of gene pools and their degree of connectivity. *Mol Ecol* 15:1519–1439.
47. Hare MP, et al. (2011) Understanding and estimating effective population size for practical application in marine species management. *Conserv Biol* 25:438–449.
48. Özturk B (1996) *Proceedings of the First International Symposium on the Marine Mammals of the Black Sea* (UNEP, Istanbul, Turkey).
49. Hall TA (1999) BioEdit: A user-friendly biological sequence alignment, editor and analysis program for Windows 95/98/ NT. *Nucleic Acids Symposium Ser (Oxf)* 41:95–98.
50. Bandelt HJ, Forster P, Röhl A (1999) Median-joining networks for inferring intraspecific phylogenies. *Mol Biol Evol* 16(1):37–48.
51. Tajima F (1989) Statistical method for testing the neutral mutation hypothesis by DNA polymorphism. *Genetics* 123:585–595.
52. Fu YX (1997) Statistical tests of neutrality of mutations against population growth, hitchhiking and background selection. *Genetics* 147:915–925.
53. Librado P, Rozas J (2009) DnaSP v5: A software for comprehensive analysis of DNA polymorphism data. *Bioinformatics* 25:1451–1452.
54. Weir BS, Cockerham CC (1984) Estimating F-statistics for the analysis of population structure. *Evolution* 38:1358–1370.
55. Hudson RR, Slatkin M, Maddison WP (1992) Estimation of levels of gene flow from DNA sequence data. *Genetics* 132:583–589.
56. Hudson RR (2000) A new statistic for detecting genetic differentiation. *Genetics* 155: 2011–2014.
57. Fontaine MC, Galan M, Bouquegneau JM, Michaux JR (2006) Efficiency of fluorescent multiplex polymerase chain reactions (PCRs) for rapid genotyping of harbour porpoises *Phocoena phocoena* with 11 microsatellite loci. *Aquat Mamm* 32:301–304.
58. Goudet J (2001) FSTAT, a program to estimate and test gene diversities and fixation indices (version 2.9.3). Available at http://www2.unil.ch/popgen/softwares/fstat.htm. Accessed July 1, 2011.
59. Rousset F (2008) genepop'007: A complete re-implementation of the genepop software for Windows and Linux. *Mol Ecol Resour* 8:103–106.
60. Raymond M, Rousset F (1995) GENEPOP (version 1.2) population genetic software for exact tests and ecumenicism. *J Hered* 86:248–249.
61. Pritchard JK, Stephens M, Donnelly P (2000) Inference of population structure using multilocus genotype data. *Genetics* 155:945–959.
62. Falush D, Stephens M, Pritchard JK (2003) Inference of population structure using multilocus genotype data: Linked loci and correlated allele frequencies. *Genetics* 164: 1567–1587.
63. Evanno G, Regnaut S, Goudet J (2005) Detecting the number of clusters of individuals using the software STRUCTURE: A simulation study. *Mol Ecol* 14:2611–2620.
64. Beaumont MA (2010) Approximate Bayesian computation in evolution and ecology. *Annu Rev Ecol Evol Syst* 41:379–406.
65. Hasegawa M, Kishino H, Yano T (1985) Dating of the human-ape splitting by a molecular clock of mitochondrial DNA. *J Mol Evol* 22(2):160–174.
66. Palsbøll PJ, Bérubé M, Aguilar A, Notarbartolo-Di-Sciara G, Nielsen R (2004) Discerning between recurrent gene flow and recent divergence under a finite-site mutation model applied to North Atlantic and Mediterranean Sea fin whale (Balaenoptera physalus) populations. *Evolution* 58:670–675.
67. Posada D (2008) jModelTest: Phylogenetic model averaging. *Mol Biol Evol* 25: 1253–1256.
68. Verdu P, et al. (2009) Origins and genetic diversity of pygmy hunter-gatherers from Western Central Africa. *Curr Biol* 19:312–318.
69. Gelman A, Carlin JB, Stern HS, Rubin DB (1995) *Bayesian Data Analysis* (Chapman & Hall, London).